

RESEARCH ARTICLE

WILEY

Characterization of CBD oils, seized on the Belgian market, using infrared spectroscopy: Matrix identification and CBD determination, a proof of concept

Céline Duchateau^{1,2} | Caroline Stévigny¹ | Kris De Braekeleer¹  | Eric Deconinck^{1,2} 

¹Pharmacognosy, Bioanalysis and Drug Discovery Unit, RD3, Faculty of Pharmacy, ULB, Brussels, Belgium

²Medicines and Health Products, Scientific Direction Physical and Chemical Health Risks, Sciensano, Brussels, Belgium

Correspondence

Deconinck Eric, Medicines and Health Products, Scientific Direction Physical and Chemical Health Risks, Sciensano, Brussels, Belgium.

Email: eric.deconinck@sciensano.be

Abstract

The availability of cannabidiol (CBD) oil products has increased in recent years. No analytical controls are mandatory for these products leading to uncertainties about composition and quality. In this paper, a methodology was developed to identify the oil matrix and to estimate the CBD content in such samples, using mid-infrared and near-infrared spectroscopy. Different oils were selected based on the information labeled on products and were bought in food stores in order to create a sample set with a variety of matrices. These oils were spiked with CBD to obtain samples with CBD levels from 0% to 20%. The first part of the study was focused on the qualitative analysis of the oil matrix. A classification model, based on Soft Independent Modeling of Class Analogy, was built using the spiked oils to distinguish between the different oil matrices. For both spectroscopic techniques, the sensitivity, the specificity, the accuracy and the precision were equal to 100%. These models were applied to determine the oil matrix of seized samples. The second part of the study was focused on the quantitative estimation of CBD. After determination of CBD in seized samples using gas chromatography-tandem mass spectrometry, partial least square regression (PLS-R) models were built, one for each matrix in the sample set. Both techniques were able to classify unknown oily samples according to their matrix, and although only few samples were available to evaluate the PLS-R models, the approach clearly showed promising results for the estimation of the CBD content in oil samples.

KEYWORDS

CBD oils, classification, MIR, NIR, regression

1 | INTRODUCTION

Cannabis sativa L. is already used for a long time for multiple applications such as traditional medicine and agricultural applications.¹ This plant of the Cannabaceae family is able to biosynthesize not less than

565 chemical compounds including terpenophenolic compounds, the so-called cannabinoids. These compounds accumulate mainly in the glandular trichomes of the female plant.² To date, 177 phytocannabinoids have been identified among which the two well-known cannabinoids, to which medical properties or health claims are assigned: the psychoactive substance Δ^9 -tetrahydrocannabinol (THC) and cannabidiol (CBD).³ They are synthesized as carboxylic acids and

Kris De Braekeleer and Eric Deconinck contributed equally as project leaders.

decarboxylated to the neutral form during exposure to light, heat, or prolonged storage; Δ^9 -tetrahydrocannabinolic acid (THCA) is decarboxylated to THC, and cannabidiolic acid (CBDA) is decarboxylated to CBD.⁴

Cultural, social, and political legal opinions regarding the use of cannabis products have been altered due to the abundance of (presumed) pharmacological activities.⁵ Thereby, CBD hemp was produced and is becoming a major commodity crop in the United States.⁶ Medical cannabis is cultivated under controlled environmental conditions in order to have a higher standardization of the cultivation process.⁷

Worldwide, the availability of oils enriched in CBD on Internet, in pharmacy, in shops, and so on has increased in recent years.^{8,9} Several companies produce and distribute CBD-based products (e.g., CBD oils) since CBD is not a controlled substance in the European Union, in contrast to THC. Due to lack of regulation, no analytical controls are mandatory for these products leading to uncertainty about the composition and quality of the products offered to the consumers.⁵ On websites, these products claim lots of benefits on different diseases such as epilepsy, pain, sleep disorders, digestive disorders.

CBD oils for medical use were first introduced in the United States of America at the end of the 90s and in Canada in 2018.¹⁰ The first oral CBD oil (Epidyolex[®]) approved by the European Medicine Agency (EMA) in 2019 was used as adjunctive therapy for seizures associated with Lennox–Gastaut syndrome combined with the drug clobazam.¹¹

Next to the registered medicinal products, a whole series of CBD oils can be found on the market and are most often based on hemp seed oil, obtained from the extraction of seeds of different chemotypes of *Cannabis sativa* L.⁵ In short, two CBD oils categories have to be distinguished here: The CBD enriched hemp seed oils and the other vegetal oils to which CBD is added. However, the origin of oils used as matrices are often doubtful and may be falsified or contaminated by other oils, according to the cost or the availability.

Some cannabis oils contain other cannabinoids than CBD and therefore also Δ^9 -THC depending on the cannabis variety used for the extraction.^{10,12} Indeed, the U.S. Federal Drug Administration (FDA) mentioned that some companies manufactured and sold cannabis-derived products that are not compliant to the “Food, Drug and Cosmetic act” and that they might put the health and safety of consumers at risk.¹³

Different methods exist¹⁴ to prepare CBD oils. The cannabinoid content may vary according to the production process. Parameters like temperature and extraction time affect the quality of the cannabis macerated oils.^{15,16} Correct storage conditions are critical for the cannabinoids content. Degradation products as CBN could be formed under the stability conditions described by Kosovic et al.¹⁷ Pavlovic et al. assessed the overall quality of CBD oil preparations by chromatographic methods and results presented notable differences in the overall cannabinoids profiles justifying the necessity to provide strong regulation and control.⁵

Conventional methods used to quantify CBD in oils are chromatographic techniques including gas chromatography coupled to

mass spectrometry (GC–MS) and liquid chromatography coupled to an UV (LC–UV) or a mass spectrometric detector (LC–MS).^{16–19} Although these methods are accurate and sensitive, they are slow and expensive and require a complete sample preparation without forgetting the requirement of trained personnel.²⁰ Mid-infrared (MIR) and near-infrared (NIR) analysis are non-destructive, fast, and green techniques and have been used across various fields.^{21,22} The combination of spectroscopic techniques with chemometrics provides a powerful tool for the interpretation and analysis of spectra and has demonstrated a great potential in the analysis of plant natural products.²³ Moreover, in connection with a part of this work, classification models were already used to discriminate different kind of oils between them.²⁴ Especially the use of attenuated total reflectance (ATR) sampling with MIR is described as one of the main methods used for liquid analysis by infrared spectroscopy.²⁵ NIR using transmittance, reflectance, and transmittance is a promising option to evaluate the quality of oilseeds and edible oils.²⁶ Chen et al. determined CBD in hemp oil by NIR spectroscopy in reflectance mode coupled to chemometrics.²⁷

This study describes an application of NIR and MIR spectroscopies combined with chemometrics to classify samples, according to the oil matrix used and to estimate the CBD content in these samples. For the latter, NIR spectra, MIR spectra, NIR and MIR concatenated spectra, and MultiBlock Partial Least Squares Regression (MB-PLS-R) were compared between them. Indeed, data were obtained by two distinct sources (NIR and MIR spectroscopies) to reach a better understanding of the physico-chemical properties of the analyzed oily samples.²⁸ In this case, the data is multi-modal and multi-source and not simply multivariate. In the current study, the modes are represented by the two different spectroscopic techniques and spectral profiles are multivariate.

2 | MATERIAL AND METHODS

2.1 | Materials

2.1.1 | Oils for spiking

Three kinds of oils were selected based on the information labeled on the CBD oil products. They were purchased in different food stores: three different brands of hemp seed oils, three different brands of olive oils, and three different brands of pumpkin seeds oils. These were stored at room temperature (20°C).

2.1.2 | Reagents and chemicals

CBD to spike the different oils was purchased from Fagron (Nazareth, Belgium, purity 98.4% m/m).

Sodium chloride was purchased from Chem-Lab (Zedegem, Belgium), sodium hydroxide 1 M, *n*-hexane, sodium sulfate, and hydrogen chloride (HCl) solution 0.5 M in methanol were purchased from Sigma-Aldrich (Darmstadt, Germany). Ultrapure Water was

obtained using a milli-Q system from Merck Millipore (Bedford, MA, USA).

2.1.3 | Preparation of spiked oils

Six concentration levels of CBD were chosen according to the availability of samples on the market and according to the solubility of CBD in oil: 0% w/w, 2% w/w, 5% w/w, 10% w/w, 15% w/w, and 20% w/w. Samples were prepared directly in glass vials by weighing the respective mass of CBD and the necessary amount of oil matrix. CBD was solubilized using sonication.

2.1.4 | Seized oil samples

Seventeen CBD oil samples were seized by the Belgian authorities in different shops. Samples were kept at room temperature before analysis, and sample codes were assigned to them. Samples are mixtures of different oils or/and hemp extracts. Some samples are labelled as “full spectrum CBD oil.” This is an extract containing all the compounds found in the hemp plant as terpenes, flavonoids, and other cannabinoids.²⁹

2.2 | Spectroscopic methods

All spiked and seized oil samples were measured in triplicate using a Frontier MIR/NIR Spectrometer™ (PerkinElmer™, USA). The averages of the spectra for each sample were used for further data analysis.

2.2.1 | MIR spectra—reflectance

Spectra were measured using the Universal ATR Reflectance Accessory with a resolution of 4 cm⁻¹. Sample was placed on top of a diamond crystal with a high refractive index. Then pressure is applied to ensure a good contact between the sample and the crystal.

Each spectrum was recorded in the region of 400–4000 cm⁻¹ and averaged across 32 scans. Background spectra were collected when no pressure was applied to the crystal. The background was recorded between each sample.

2.2.2 | Near infrared spectra—transflectance

Spectra were measured in transflectance mode with a resolution of 8 cm⁻¹. The sample was placed into the sample dish and covered by the liquid transflectance accessory.

Each spectrum was recorded in the region of 10,000–4000 cm⁻¹ and averaged across 16 scans. Background spectra were collected with a reflector provided by PerkinElmer™. The background was recorded between each sample.

Spectra were also measured using the NIR Reflectance Accessory in diffuse reflectance mode but the spectral data obtained seemed inferior and results in chemometrics were much better in transflectance mode. Therefore, these results were not discussed in the presented paper.

2.3 | Oily matrix analysis: GC–MS and sample preparation procedure

The seized oil samples were analyzed by an inhouse GC–MS method to identify the composition of the matrix. Each seized sample was analyzed only once due to the small volume of samples available.

The assay solution was prepared as follows: 300 mg of the seized oil sample was dissolved and diluted to 10.0 mL with *n*-hexane. After homogenization, 2.5 mL of this solution was dried under a nitrogen stream. The residue was dissolved in a mixture of 2.5 mL HCl 0.5 M methanolic solution and 2.5 mL of *n*-hexane, using vortex (1 min) and heating in an oven at 80°C for 30 min. After cooling, 2.5 mL sodium hydroxide 0.5 M, 2.5 mL of *n*-hexane, and 0.5 g of NaCl were added to the mixture (vortex 1 min). The organic layer was separated, and anhydrous sodium sulfate was added. The solution stands for 5 min, and the supernatant was diluted 10 times with *n*-hexane; 1 mL was placed in a GC–MS vial.

Fatty acids were analyzed using a Thermo Scientific Trace GC Ultra with DSQ II GC–MS system (Thermo Fischer Scientific, Austin, USA) equipped with a SP-2560 capillary highly polar GC column (fused silica L 100 m × I.D. 0.25 mm × d_f 0.20 μm, Sigma-Aldrich, Darmstadt, Germany). The injector temperature was 230°C with an injection volume of 1 μL in split mode (1/50). The carrier gas (He) flow rate was set at 1.5 mL/min. The temperature gradient started at 50°C which was held for 1 min. Then, the temperature was linearly increased to 250°C at a rate of 20°C/min and held for 4 min. Finally, the temperature was linearly increased to 290°C at a rate of 20°C/min and held for 3 min. The MS detector temperature was set at 280°C. The device was controlled by Thermo Xcalibur software (software version 3.1).

The fatty acids in the extract were identified by matching the mass spectrum with the National Institute Standard Technology (NIST). The required matching was achieved with a match factor thresholds >900 NIST library guidelines. More the match factor is high, better is the mass spectral match.

Based on the fatty acid composition, olive oil, hemp seed oil, and pumpkin seed oil were identified. The following composition of fatty acids was found in the literature.^{30–33} Oleic acid: 76% (olive), 10%–16% (hemp seed), and 29%–41% (pumpkin seed); linoleic acid: 1%–8% (olive), 50%–70% (hemp seed), and 44%–52% (pumpkin seed); α-linolenic acid: almost absent in olive and pumpkin seed and 15%–25% for hemp seed. The identification was not always straightforward due to the presence of degradation products, like for instance pentadecanoic acid which is an oxidation product of linoleic acid and linolenic acid or heptanoic acid which is an oxidation product of oleic acid.³⁴

The determination of the CBD content of the seized samples was performed following the GC-MS/MS method described previously by our group.³⁵

2.4 | Chemometrics

2.4.1 | Software

Chemometric analysis was performed using the PLS_toolbox (Eigenvector Research, WA, USA) with Matlab version R2020b (The Mathworks™, Natick, USA).

2.4.2 | Data preprocessing

Single-block data analysis

Several pretreatment techniques and different combinations were applied on the raw MIR and NIR spectra. The first derivative, using the Savitsky-Golay algorithm with window size of 15 and a second order polynomial was used to correct the baseline drift.

Multi-block data analysis

To investigate the complementarity of the information obtained from the two spectroscopic techniques, the preprocessed NIR and MIR spectral profiles were concatenated³⁶ and analyzed by SIMCA and PLS-R.

MB-PLS-R³⁷ was applied after block variance scaling (inter-block preprocessing) and first derivative, using the Savitsky-Golay algorithm with window size of 15 and a second order polynomial was used to correct the baseline drift (intra-block preprocessing).

2.4.3 | Unsupervised analysis—principal component analysis (PCA)

PCA is commonly used to perform exploratory data analysis of spectral data. PCA reduces the dimensions of the original data space into latent variables called principal components to show the similarities and differences between the spectra.^{38,39}

2.4.4 | Kennard and Stone algorithm

The Kennard and Stone algorithm was applied to select a training and a validation set.³⁹ The training set was used to generate the model, and the validation set was selected to perform validation of the prediction capacity of the model. The Kennard and Stone method selects samples (spectra) in the validation set sequentially based on a distance measure, starting with the spectrum closest to the mean spectrum. The next sample is situated furthest away from the first one. The third selected is the most distant one from the samples selected in the validation set. The selection continues until a predefined number of samples is selected in the validation set. The remaining samples are included in the training set.

2.4.5 | Supervised analysis

Soft independent modelling of class analogy (SIMCA)

SIMCA is a supervised classification technique that uses samples with known origin to define a decision rule, which allows to classify new samples with unknown origin. Each class is modelled individually by

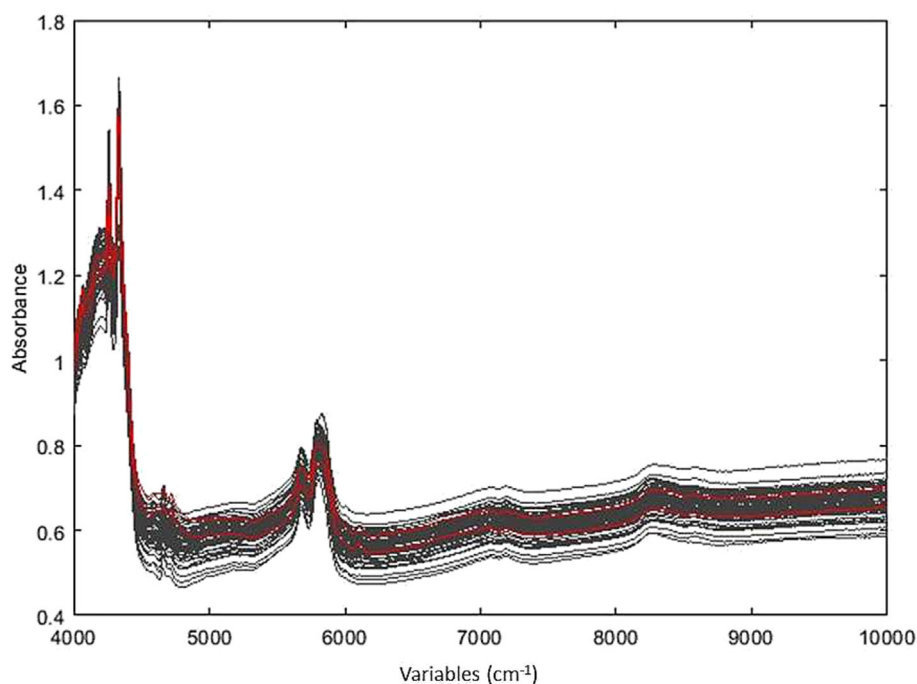


FIGURE 1 NIR absorbance raw spectra in the wavenumber region 10,000–4000 cm^{-1} .

PCA. The number of PCs of each class of the training set (spiked samples) was selected by venetian blinds cross validation.⁴⁰ Statistical parameters used to evaluate the model were: sensitivity, specificity, accuracy, and precision.

Partial least square regression (PLS-R)

In PLS-R, latent variables are defined as linear combinations of the manifest variables. These combinations or PLS factors are selected to maximize the amount of variation explained in the spectral data that is relevant for predicting the concentration of CBD.⁴¹ The number of latent variables (LVs) was selected by venetian blinds cross validation. PLS-R searches for the maximum co-variance between the spectra and the concentrations. Quality measures of the PLS-R models are as

follows: the root mean square error for calibration (RMSEC), cross validation (RMSECV) and validation set (RMSEP), the determination coefficient R^2 between predicted and real values for, respectively, calibration ($R^2_{(cal)}$), cross-validation ($R^2_{(CV)}$), and validation set ($R^2_{(p)}$) and the absolute errors of residuals for the samples of the validation set.

MB-PLS-R

SIMCA and PLS-R (single-block chemometrics techniques) were used for single-mode data generated by a single analytical technique and for the simple concatenated NIR and MIR spectra before chemometrics. For the concatenated data, these techniques extract only a limited part of the information. This is the reason why

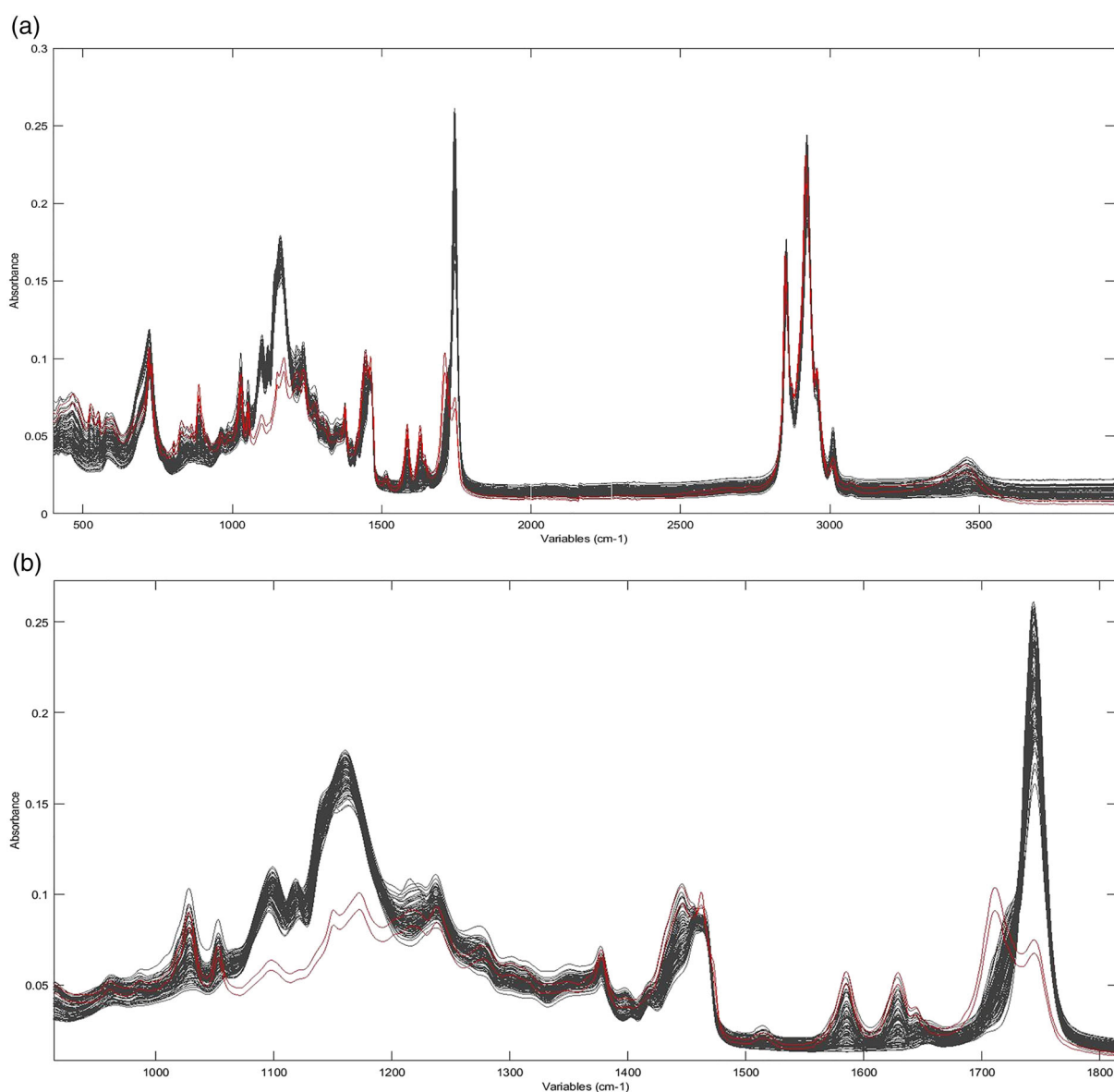


FIGURE 2 MIR absorbance raw spectra in the wavenumber region 10,000–4000 cm^{-1} showing two deviating seized samples spectra in red (a) and a close-up look at this deviating part (b).

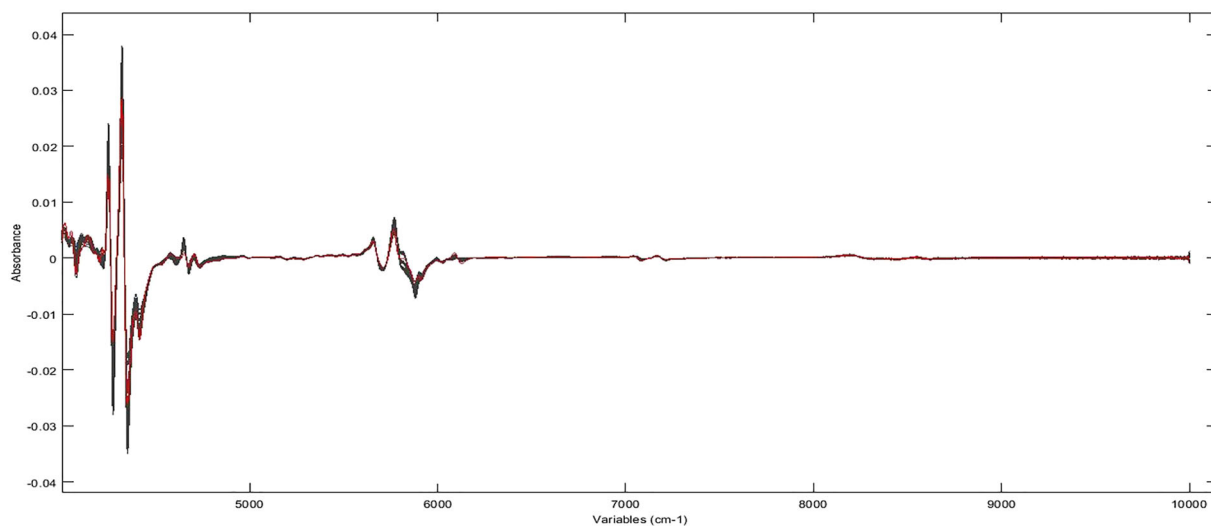


FIGURE 3 NIR spectra after the first derivative.

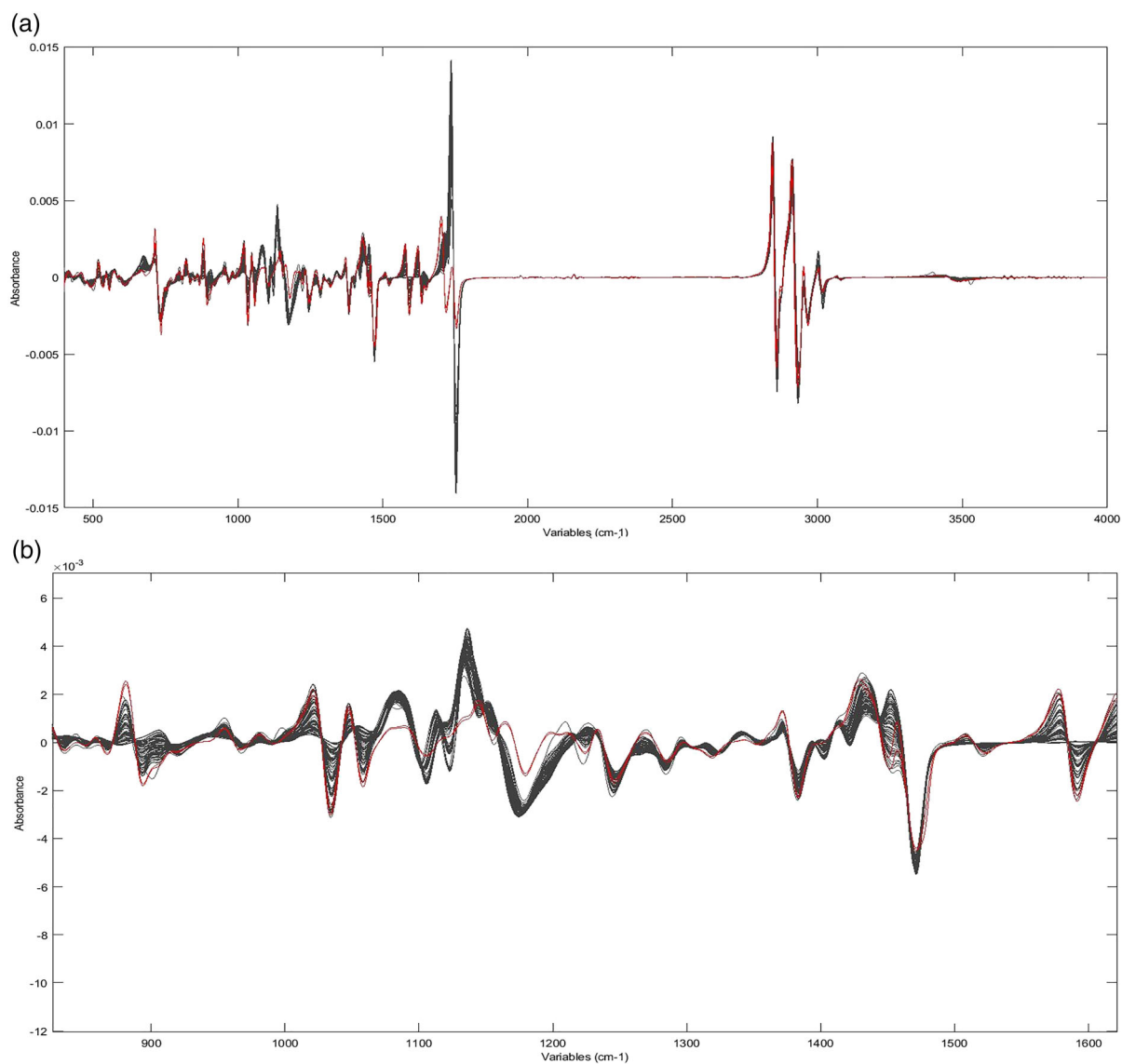


FIGURE 4 MIR spectra after the first derivative showing two deviating seized samples in red (a) and a close-up look at this deviating part (b).

multi-block data analysis techniques were used to extract more information from the data generated by the multiple modes to improve the quality of the models. This approach maximizes the covariance with the response variables and allows the extraction of global scores.²⁸

3 | RESULTS AND DISCUSSION

3.1 | Preprocessing

A NIR matrix (54×3001) and a MIR matrix (54×3601) of the spiked oils (3 types of oil \times 3 brands of oil \times 6 concentration levels = 54 spectra) and a NIR matrix (17×3001) and a MIR matrix (17×3601) for the seized samples (17) were created. Seized samples were previously analyzed by GC-MS (see Section 2.3) to identify the fatty acids and to check the label claim. NIR raw spectra are shown in Figure 1. Figure 2a shows the MIR raw spectra. On the figures, two seized samples (spectra colored in red) have a deviating fingerprint. Figure 2b proposes a close-up look at the deviating part because the deviation of the two seized samples (colored in red) is more pronounced for MIR. The pretreated spectra are shown in Figure 3 for NIR and in Figure 4a,b (close-up look at the deviating part) for MIR. The composition for one of the outlier samples was clearly different. Figure 5 represents a chromatogram showing hemp seed oil, olive oil, and pumpkin seed oil, and the two outlying samples. For one outlier, the highest peak was matched with myristinoyl glycinamide, and another peak was matched with eicosanoic acid, a major constituent of peanut oil. For the other outlier, the presence of linoleic acid and α -linolenic acid implies the presence of hempseed oil, but for both outliers, an unknown compound is present at 19 min and the peak at 8 min is totally absent.

3.2 | PCA

The seized samples with deviating fingerprint were also observed in the PCA plot and were removed before supervised analysis. Figure 6a shows the PCA plot for the NIR data with the outlying samples in red, and Figure 6b shows the PCA plot for NIR data without the outlying samples showing clearly the separation of the samples according to the oil matrix. Figure 7a,b shows the PCA plot for the MIR data before and after the removal of the deviating profiles. These figures show clearly the separation of the samples according to the oil matrix. Hemp-based oils (■) were separated from olive-based oils (▲). Pumpkin-based oils (▼) were situated between them.

Both spectroscopic techniques show the same results and the first three PCs explain more than 99% of the total variance.

The loadings for the first three PCs were explored in order to identify the most specific regions linked to the oil matrix and the CBD concentration. Siano et al. compared the chemical characteristics and ATR-MIR analysis of hemp-based oils samples.⁴² The typical carbonyl (C=O) band from carboxylic acid of fatty acids contained in lipids is shown at 1744 cm^{-1} . The generic structure of fatty acids is $\text{CH}_3\text{-(C}_x\text{H}_y)_n\text{-COOH}$.⁴³ In addition from this bands, hydrogen/carbon (C-H) bond due to the lipid content in oil is shown in the region of $2700\text{--}3010 \text{ cm}^{-1}$. Carbohydrates possess strong and characteristic IR absorptions between 1200 and 750 cm^{-1} and are normally missing in oil. Figure 8 represents the loadings according to PC3 showing these spectral regions. The loadings on PC1 and PC3 are almost identical, yet the loading of the carbonyl (C=O) band at 1744 cm^{-1} is very high on PC1 (Figure 9).⁴⁴ For the NIR spectra, lipids are shown at 5780 cm^{-1} , 5681 cm^{-1} , 4300 cm^{-1} , and 4255 cm^{-1} while aromatic hydrocarbons present in cannabinoids, like CBD, are typically present at 6000 cm^{-1} .⁴⁵ Figure 10 represents the plot of loadings according to PC3 showing the spectral regions of lipids (C=O bands), and

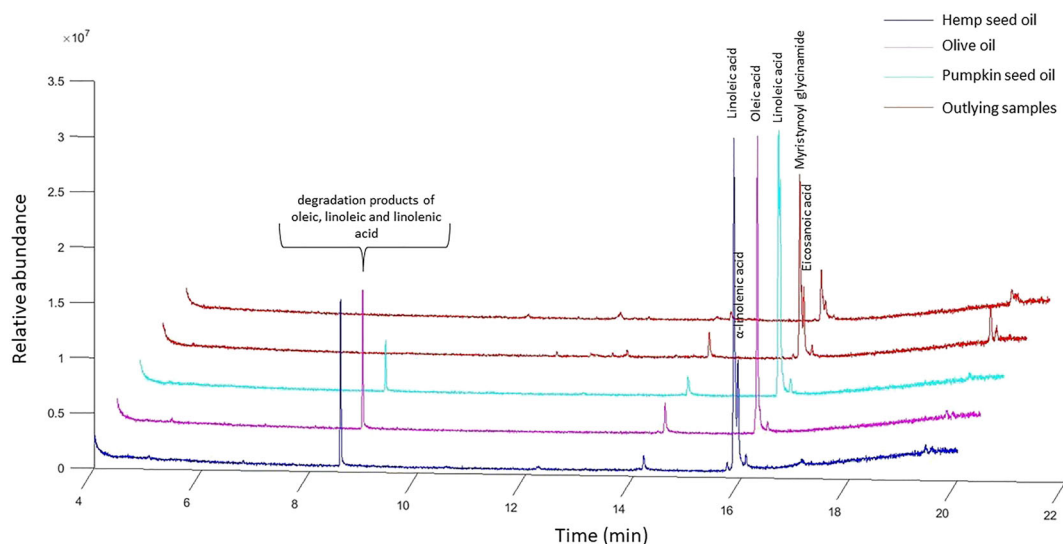


FIGURE 5 Chromatogram of GC-MS method showing fatty acids pics in various type of oils indicated with different colors depending on the matrix: hemp seed oil (dark blue), olive oil (fuchsia), pumpkin seed oil (cyan), and the two outlying samples (red).

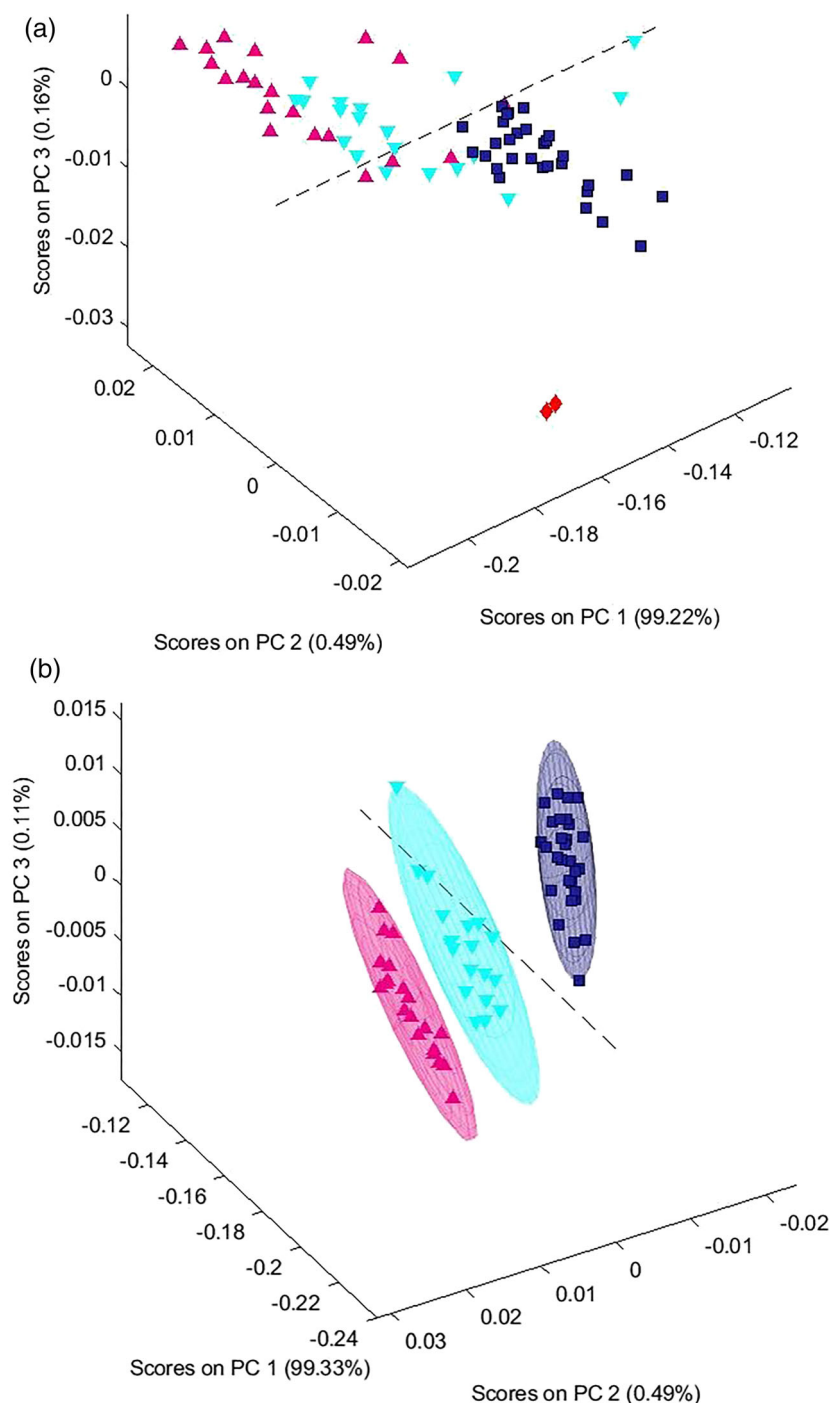


FIGURE 6 PCA plot obtained with the NIR spectra. Samples are indicated with different colors depending on the oil matrix: hemp seed oil (■), olive oil (▲), pumpkin seed oil (▼), and the two outlying samples (◇) (a). PCA plot without the two outlying samples and various matrices grouped in ellipses (b).

Figure 11 shows the plot of loadings according to PC1, which may be related to the CBD signal. Performing PCA analysis with only the selected regions did not improve the separation.

3.3 | Supervised analysis

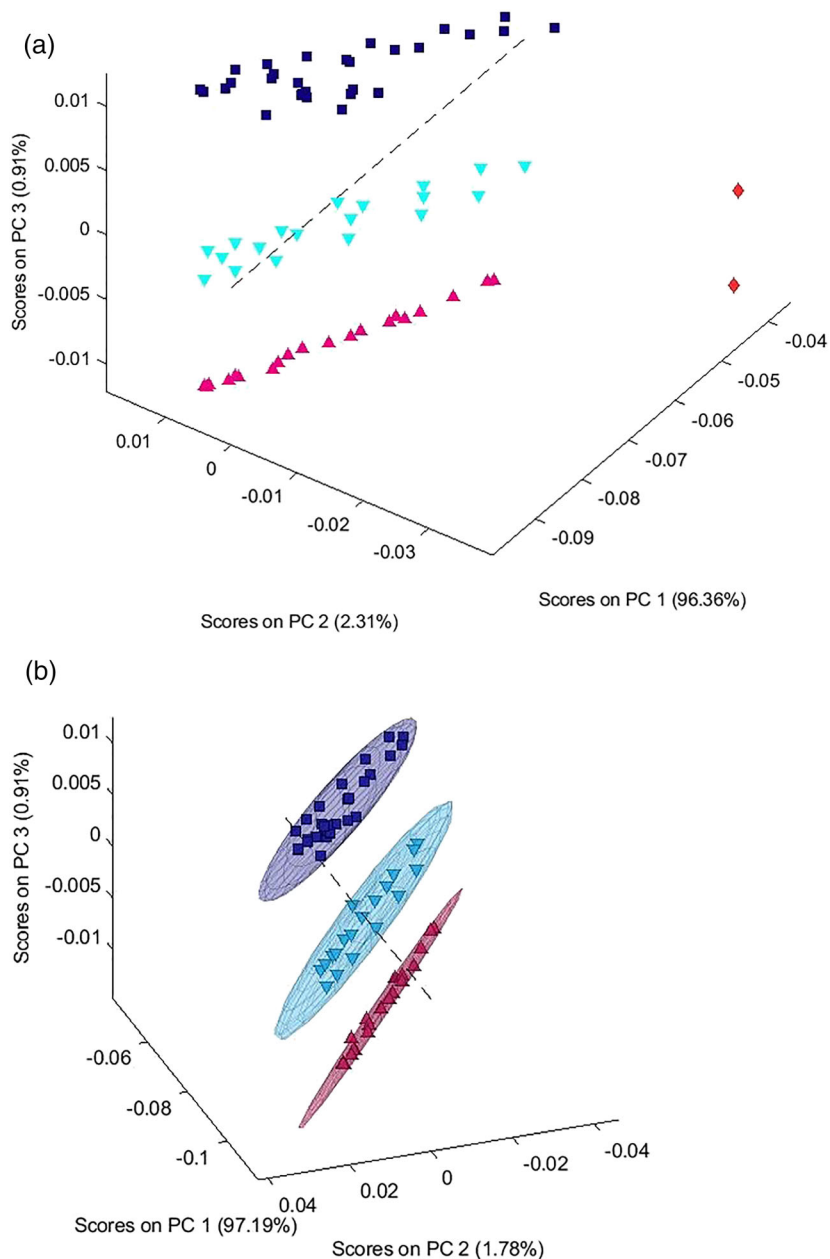
The two seized samples considered as outliers (Section 3.1) were excluded after PCA analysis and were not considered for SIMCA and PLS-R.

3.3.1 | SIMCA

Before modelling, Kennard and Stone was used to select 16 spiked CBD oils as a validation set. The 38 remaining spiked CBD oils formed the training set.

Classification models were created by attributing a class to each of the respective oil matrices under consideration. The first class represents hemp seeds oil, the second class olive oil, and the third pumpkin seeds oil. Statistical values obtained with SIMCA for NIR and MIR are shown in Table 1.

FIGURE 7 PCA plot obtained with the MIR spectra. Samples are indicated with different colored symbols depending on the oil matrix: hemp seed oil (■), olive oil (▲), pumpkin seed oil (▼), and the two outlying samples (◇) (a). PCA plot without the two outlying samples and various matrices grouped in ellipses (b).



Each sample of the validation set was attributed to one of the three classes. The accuracy was 100% for the training set (cross validation) and for the validation set for both NIR and MIR.

The classification model was applied to predict the 15 remaining seized oil samples. Results are shown in Table 2. Each seized sample was attributed to one of the three classes and the predicted class corresponded with the label claim and the analysis of fatty acids by GC-MS. The color of the seized samples with the same label claim was not always the same. For instance, CBD 1 and CBD 2 have not the same color than CBD 5 and CBD 6. Nevertheless these four seized samples are labelled with hemp seed oils and hemp extract. Probably, the difference in color is due to the extract added in the hemp seed oil or due to natural variation. The difference in color has no impact on the classification of the NIR and MIR spectra.

3.3.2 | PLS-R

In order to estimate the amount of CBD, PLS-R models were built for each oil matrix: hemp seed oil, olive oil, and pumpkin seed oil. The seized samples were analyzed using GC-MS/MS according to a method developed previously by our group³⁵ and used in this research as reference method. The chromatographic results and label claims are shown in Table 3.

Table 4 gives an overview of the statistical values (Section 2.4.5) obtained with PLS-R for NIR and MIR spectra, concatenated NIR-MIR spectra, and MB-PLS-R. The statistical parameters shown in the table are R^2 between predicted and real values for, respectively, $R^2_{(calibration)}$, $R^2_{(CV)}$ and validation set ($R^2_{(p)}$), RMSEC, RMSECV, and RMSEP, and the absolute errors or residuals for the samples of the validation set.

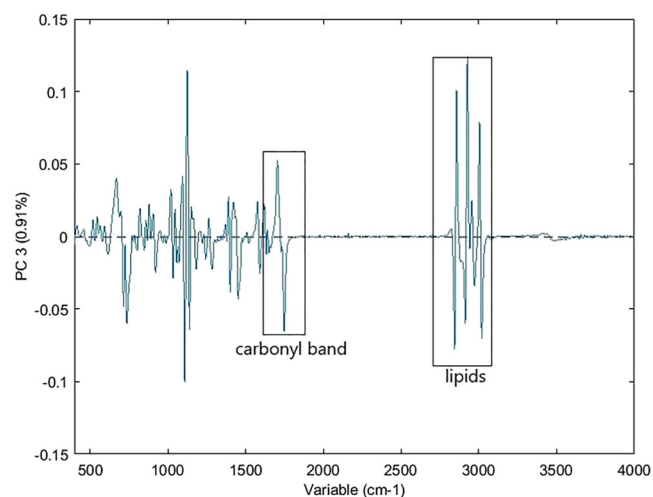


FIGURE 8 Average of loadings according to PC3 obtained with MIR spectra showing the carbonyl and lipids bands in boxes.

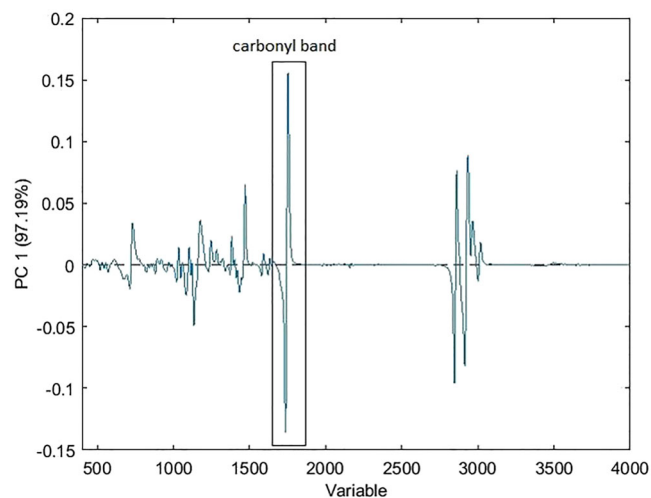


FIGURE 9 Average of loadings according to PC1 obtained with MIR spectra showing the carbonyl band in box.

These values are given for information. Due to the high variability in the seized sample set compared to the spiked sample set, it was decided to combine both matrices and to select training set and validation set on the matrix. The Kennard and Stone algorithm selected 25% of samples in the validation set. The number of samples used for each set is described in the table as well as the sample code of samples used for the validation set. Attention was paid to include also seized samples in the validation set. Since for the pumpkin seed oil only one seized sample was available, this one was selected for the validation set. The discussion hereunder is mainly focused on the values for the validation set, since these are the most important, pointing at the overall reliability and robustness of the model.

For the olive oil model, very comparable results could be obtained for both the NIR and the MIR spectra, as well as for the concatenated

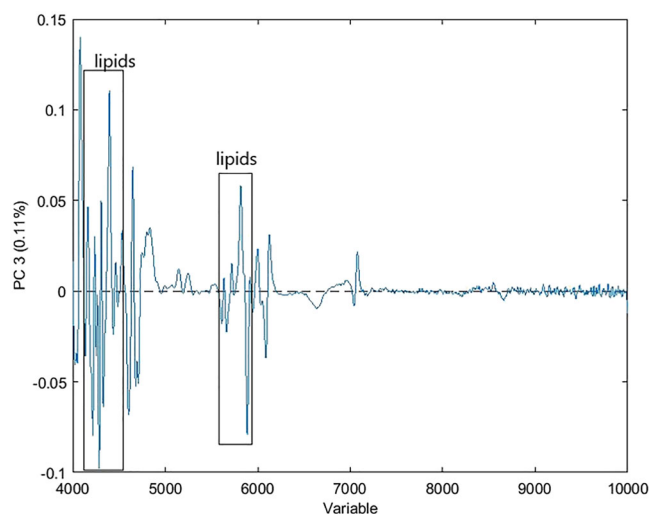


FIGURE 10 Average of loadings according to PC3 obtained with NIR spectra showing the lipids bands band in boxes.

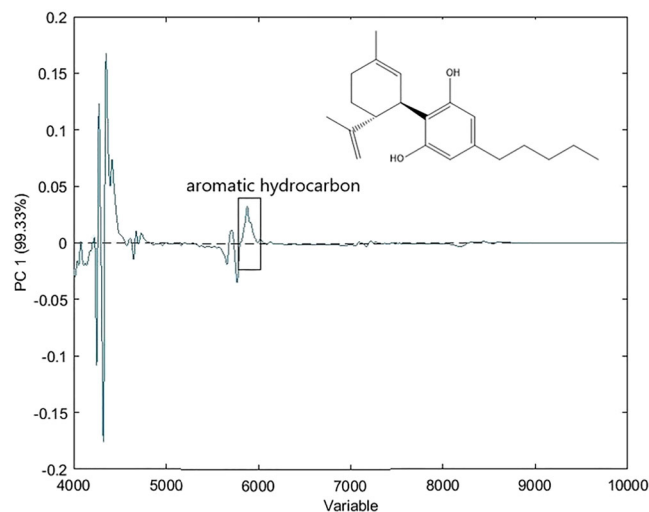


FIGURE 11 Average of loadings according to PC1 obtained with NIR spectra showing the aromatic hydrocarbon (from CBD) in box. The chemical structure of CBD is shown in the upper right corner.

NIR and MIR spectra. The NIR-MIR MB PLS-R model shows the smallest value for RMSEC and for RMSECV indicating that these model fits the data best. However, NIR and MIR (single block) models require fewer factors than the other models for the same data, which is advantageous in both model implementation and model interpretation. For the prediction on new samples, with RMSEP values of, respectively, 0.9 for NIR, 1.7 for MIR, 1.8 for concatenated NIR-MIR spectra, and 3.0 for MB-PLS-R, models were able to estimate quite closely the CBD content in olive oil. Overall, the best model for olive oil is obtained with NIR with its RMSEP value of 0.9 and a maximal residual for the validation set of 1.3%. For this data set, it seems that the combination of data obtained with both techniques did not result in better models compared to the individual techniques.

A different view was obtained for the hemp seed oil. Here, it can be observed that the RMSEP value for the NIR model is higher than those of the other models (RMSEP of 3). This is also reflected by the

TABLE 1 Statistical values obtained with SIMCA for NIR and MIR spectra.

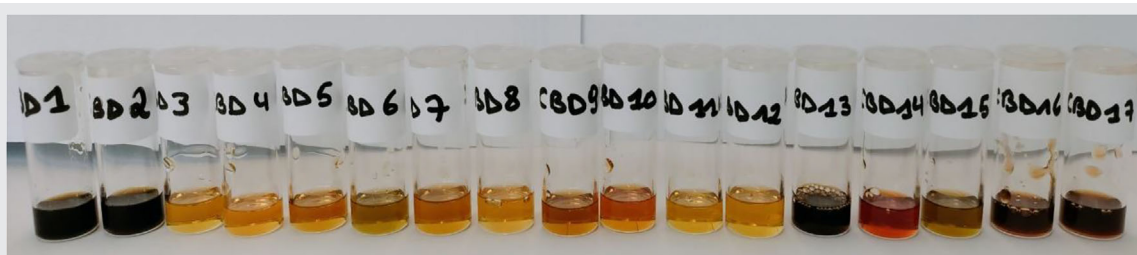
Spectroscopic technique	NIR	MIR
Devices preprocessing	1st derivative	1st derivative
SIMCA		
Model building: Training set		
Number of PC's for each classes (venetian blinds)	2-3-3	4-3-3
Sensitivity	1.00-1.00-1.00	1.00-1.00-1.00
Specificity	1.00-1.00-1.00	1.00-1.00-1.00
Accuracy	1.00-1.00-1.00	1.00-1.00-1.00
Precision	1.00-1.00-1.00	1.00-1.00-1.00
Model building: Validation set		
Sensitivity	1.00-1.00-1.00	1.00-1.00-1.00
Specificity	1.00-1.00-1.00	1.00-1.00-1.00
Accuracy	1.00-1.00-1.00	1.00-1.00-1.00
Precision	1.00-1.00-1.00	1.00-1.00-1.00

residuals obtained for the external validation set. The hemp seed model, which is the most trustworthy model, due to a significantly higher number of seized samples included, clearly shows that much better estimations can be obtained with MIR with a maximum residual of 2.5%. The maximum residuals was 3.6% for NIR and 5.5% for concatenated NIR-MIR spectra. The second best model is the one based on the MB-PLS-R using both NIR and MIR spectra. Here, the lowest RMSECV and RMSEP values could be obtained of, respectively, 2.8 and 1.6, though the maximal residual for the validation set was here 3.5%, which is significantly higher than the one obtained with MIR alone. Again, it could be observed that the combination of techniques had no added value for modelling this data set.

For pumpkin seed oil, no reliable models could be obtained due to the lack of seized pumpkin seed oil samples. Any seized sample could be added in the training set to increase the matrix variability. First, the only seized sample shows a residual of more than 5 for the three models, which is unacceptable. Although small values are obtained for RMSEC and for RMSECV, especially for the NIR-MIR MB-PLS-R model (with 1.0 and 1.2, respectively), the RMSEP values are unacceptable, especially for the concatenated NIR-MIR matrix with 3.9 and NIR-MIR MB-PLS-R with 3.7. Though it has to be said that here the model is only based on spiked samples, so less variability in matrix was added to the model compared to the others. This shows the

TABLE 2 SIMCA prediction results according to the label claim, the analysis of the matrix, and aspect of the sample.

Sample-code	Label claim (major ingredients constituting the matrix)	Matrix analysis	Prediction
CBD1	Hemp seed oil and hemp extract	Hemp seed oil	Hemp seed oil
CBD2	Hemp seed oil and hemp extract	Hemp seed oil	Hemp seed oil
CBD3	Full spectrum CBD oil	Hemp seed oil	Hemp seed oil
CBD4	Full spectrum CBD oil	Hemp seed oil	Hemp seed oil
CBD5	Hemp seed oil and hemp extract	Hemp seed oil	Hemp seed oil
CBD6	Hemp seed oil and hemp extract	Hemp seed oil	Hemp seed oil
CBD7	Hemp seed oil	Hemp seed oil	Hemp seed oil
CBD8	Olive oil and hemp extract	Olive oil	Olive oil
CBD9	Olive oil and hemp extract	Olive oil	Olive oil
CBD10	Full spectrum CBD oil	Hemp seed oil	Hemp seed oil
CBD11	Full spectrum CBD oil	Hemp seed oil	Hemp seed oil
CBD12	Full spectrum CBD oil	Hemp seed oil	Hemp seed oil
CBD13	Pumpkin seed oil, <i>Cannabis sativa</i> flower extract	Pumpkin or hemp seed oil	Pumpkin seed oil
CBD14	Hemp seed oil	Hemp seed oil	Hemp seed oil
CBD15	Hemp seed oil, hemp extract	Hemp seed oil	Hemp seed oil
CBD 16	Hemp seed oil, CBD extract	Hemp seed oil	Not considered, outlying sample
CBD 17	Hemp seed oil, CBD extract	Not identified	Not considered, outlying sample



	Model	CBD label claim (% w/w)	CBD GC-MS/MS (% w/w)
CBD1	Hemp	2.9	2.7
CBD2	Hemp	4.0	2.5
CBD3	Hemp	5.0	5.9
CBD4	Hemp	5.0	5.3
CBD5	Hemp	5.0	8.4
CBD6	Hemp	3.0	3.6
CBD7	Hemp	5.0	6.5
CBD8	Olive	4.0	4.5
CBD9	Olive	10.0	4.8
CBD10	Hemp	20.0	3.8
CBD11	Hemp	10.0	2.9
CBD12	Hemp	10.0	2.8
CBD13	Pumpkin	5.0	3.1
CBD14	Hemp	15.0	8.4
CBD15	Hemp	10.0	4.5

TABLE 3 Analysis of CBD oils products.

TABLE 4 Statistical values obtained with PLS-R for NIR spectra, MIR spectra, concatenated NIR-MIR spectra, and for MB PLS-R for olive oil, hempseed oil, and pumpkinseed oil models.

Spectroscopic technique	Olive oil			
	NIR	MIR	Concatenated NIR-MIR	NIR-MIR MB-PLS
Devices preprocessing	1st derivative			
Number of samples (training set)	14 spiked samples + 1 seized sample = 15 samples			
Number of samples (validation set)	4 spiked samples + 1 seized sample = 5 samples			
Number of LVs (venetian blinds)	2	2	3	3
R ² (calibration)	0.90	0.89	0.91	0.98
R ² (CV)	0.84	0.86	0.89	0.97
R ² (p)	0.98	0.94	0.96	0.88
RMSEC	2.8	3.0	2.7	1.2
RMSECV	3.7	3.3	3.1	1.6
RMSEP	0.9	1.7	1.8	3.0
Sample code	% CBD: Measured Predicted (residuals)			
HS1_10% spike	10.9 12.2 (1.3)	10.9 12.5 (1.6)	10.9 13.7 (2.8)	10.9 13.0 (2.1)
HS2_15% spike	17.4 16.6 (-0.8)	17.4 15.0 (-2.4)	17.4 16.9 (-0.5)	17.4 16.4 (-1)
HS3_2% spike	2.0 2.0 (0)	2.0 2.4 (0.4)	2.0 2.2 (0.2)	2.0 2.6 (0.6)
HS3_15% spike	16.7 16.1 (-0.6)	16.7 17.8 (1.1)	16.7 19.3 (2.6)	16.7 18.5 (1.8)
CBD8	4.5 3.2 (-1.3)	4.5 6.6 (2.1)	4.5 6.1 (1.6)	4.5 0 (-4.5)
Spectroscopic technique	Hemp seed oil			
	NIR	MIR	Concatenated NIR-MIR	NIR-MIR MB-PLS
Devices preprocessing	1st derivative			
Number of samples (training set)	14 spiked + 9 seized samples = 23 samples			
Number of samples (validation set)	4 spiked samples + 3 seized samples = 7 samples			
Number of LVs (venetian blinds)	4	5	2	2
R ² (calibration)	0.96	0.96	0.66	0.90
R ² (CV)	0.56	0.76	0.53	0.88
R ² (p)	0.86	0.90	0.84	0.94
RMSEC	1.5	1.6	4.4	2.4

TABLE 4 (Continued)

Spectroscopic technique	Hemp seed oil			
	NIR	MIR	Concatenated NIR-MIR	NIR-MIR MB-PLS
RMSECV	5.4	4.1	5.3	2.8
RMSEP	3.0	2.4	2.6	1.6
Sample code	% CBD: Measured Predicted (residuals)			
HS13_10% spike	10.9 11.3 (0.4)	10.8 12.0 (1.2)	10.9 10.2 (-0.7)	10.9 11.2 (0.3)
HS14_15% spike	17.7 17.7 (0)	17.4 18.1 (0.7)	17.1 15.1 (-2)	17.7 16.8 (-0.9)
HS15_2% spike	2.0 1.5 (-1)	1.9 2.1 (0.2)	2.0 1.6 (-0.4)	2.0 1.6 (-0.4)
HS15_15% spike	15.3 13.5 (-1.8)	15.1 15.9 (0.8)	15.3 12.5 (-2.8)	15.3 15.1 (-0.2)
CBD2	2.5 1.0 (-1.5)	2.5 1.1 (-1.4)	2.5 4.4 (1.9)	2.5 4.5 (2)
CBD6	3.6 0 (-3.6)	3.6 1.9 (-1.7)	3.6 3.8 (0.2)	3.6 2.9 (-0.7)
CBD10	3.8 6.0 (2.2)	3.8 6.3 (2.5)	3.8 9.3 (5.5)	3.8 7.3 (3.5)
Spectroscopic technique	Pumpkin seed oil			
	NIR	MIR	Concatenated NIR-MIR	NIR-MIR MB-PLS
Devices preprocessing	1st derivative			
Number of samples (training set)	15 spiked samples			
Number of samples (validation set)	4 spiked samples + 1 seized sample = 5 samples			
Number of LVs (venetian blinds)	2	3	3	2
R ² (cal)	0.91	0.96	0.98	0.94
R ² (CV)	0.86	0.96	0.96	0.92
R ² (p)	0.84	0.93	0.73	0.45
RMSEC	2.6	1.2	1.3	1.0
RMSECV	3.4	1.5	1.9	1.2
RMSEP	3.3	2.7	3.9	3.7
Sample code	% CBD: Measured Predicted (residuals)			
HS19_10% spike	11.7 13.4 (1.7)	11.6 12.5 (0.9)	11.7 12.6 (0.9)	11.7 13.0 (1.3)
HS20_15% spike	17.2 14.8 (-2.4)	17.0 17.7 (0.7)	17.2 15.9 (-1.3)	17.2 12.3 (-4.9)
HS21_2% spike	2.3 3.9 (1.6)	2.3 2.5 (0.2)	2.3 2.9 (0.6)	2.3 1.0 (-1.3)
HS21_15% spike	17.8 17.6 (-0.2)	17.5 16.2 (-1.3)	17.8 18 (0.2)	17.8 17.6 (-0.2)
CBD13	3.1 9.7 (6.6)	3.1 8.3 (5.2)	3.1 11.7 (8.6)	3.1 13.3 (10.2)

importance for the inclusion of matrix variability into the models, not only here, but generally when creating chemometrics models.

4 | CONCLUSION

NIR and MIR spectroscopy coupled to chemometrics were applied as tool to classify CBD containing oils based on their oil matrix and to estimate the CBD content. In the present study, different types of oils were spiked at different concentration levels to create a pool of samples in order to build models for classification and regression. During unsupervised analysis, both MIR and NIR allowed the discrimination between different types of oils along PC3 and showed an ascending tendency of CBD concentration according to PC1. This analysis also revealed seized samples with deviating matrix, which would interfere with the modelling and therefore were removed from the sample set.

Indeed, the GC-MS analysis confirmed, at least for one of them the total difference in composition of fatty acid and for the other seized sample the presence of undetermined components affected the samples discrimination.

Based on the promising results of the unsupervised approach, supervised analysis was conducted to classify the samples and estimate their CBD content. After the classification step, regression models were built for each type of oil to estimate the CBD content in each type of oil. For that, single-block and multi-block data analysis techniques were compared.

This study was limited by the small amount of seized oil samples, which was particularly an issue for the regression models, tempting to estimate the CBD content in the samples. In order to be routinely applicable, these regression models should be based on a large number of samples from the market, previously analyzed with standard techniques like GC-MS/MS, in order to incorporate the variation in

matrices on the market in the model. It was clearly shown in this research, since only when including part of the seized samples into the training set, acceptable results for the seized samples in the validation set could be obtained. Models based on only spiked samples resulted in significantly higher deviations.

For the classification according to the oil matrix, both techniques, NIR and MIR spectroscopy, showed comparable results. Classification techniques could be applied to check the matrix mentioned on the label claim for oily samples. In the context of the regression for estimation of the CBD content, MIR as stand-alone technique gave the best results. Regression models for CBD based on MIR could be applied to estimate the interval of concentration of samples. This conclusion is mainly based on the model for hem seed oil, for which more seized samples were available.

It was also shown that the combination of NIR and MIR data, by simple concatenation or in multi-block analysis, did not result in better models, meaning probably that for our sample set complementarity between both techniques is lacking. The fact that MIR was selected as the best option is also advantageous from a practical point of view since this facilitates on-site analysis and the implementation of the presented approach. It could be realized to sort dubious samples before analysis with an expensive reference.

The results reveal a promising tool for the fast characterization and safety evaluation of CBD containing oils, which could be broadened and exploited even more, due to the emergence of high quality portable infrared spectrophotometers. Indeed, classification and regression models could be transferred in portable devices offering the possibility to do on-site analysis. It could be useful for inspectors, distributors, and sellers. Next to oil identification and CBD content estimation, the techniques are also able to detect deviating samples, based on unexpected oils, perhaps even dangerous, and cases of deception of the consumer by either using cheaper oils than labelled or deviating CBD content compared to the label.

ACKNOWLEDGMENTS

The authors would like to thank Basma Najar and Marie Faes from RD3-PBM unit of the Faculty of Pharmacy of ULB for the technical support. We would also thank the inspectorate of the Federal Public Service for Health and Environment for providing us with the oily seized samples.

ORCID

Kris De Braekeleer  <https://orcid.org/0000-0002-3910-2990>

Eric Deconinck  <https://orcid.org/0000-0001-6980-6684>

REFERENCES

- Andre C, Hausman J, Guerriero G. Cannabis sativa: the plant of the thousand and one molecules. *Front Plant Sci.* 2016;7(19):19. doi:10.3389/fpls.2016.00019
- Elsohly M, Radwan M, Gul W, Chandra S, Galal A. Phytochemistry of *Cannabis sativa* L. In: Douglas Kinghorn A, Falk H, Gibbons S, Kobayashi J, eds. *Phytocannabinoids: Unraveling the Complex Chemistry and Pharmacology of Cannabis sativa*. 1st ed. Springer, Inc; 2017:2-30. doi:10.1007/978-3-319-45541-9
- Adamek K, Maxwell A, Jones P, Torkamaneh D. Accumulation of somatic mutations leads to genetic mosaicism in cannabis. *Plant Genome.* 2022;15(1):20169. doi:10.1002/tpg2.20169
- Bakel V, Van Bakel H, Stout J, et al. The draft genome and transcriptome of *Cannabis sativa*. *Genome Biol.* 2011;12(10):R102-R117. doi:10.1186/gb-2011-12-10-r102
- Pavlovic R, Nenna G, Calvi L, et al. Quality traits of "Cannabidiol oils": cannabinoids content, terpene fingerprint and oxidation stability of European commercially available preparations. *Molecules.* 2018;23(5):1230. doi:10.3390/molecules23051230
- Vasanth Rupasinghe HP, Davis A, Kumar S, Murray B, Zheljzkov VD. Industrial hemp (*Cannabis sativa* subsp. *sativa*) as an emerging source for value-added functional food ingredients and nutraceuticals. *Molecules.* 2020;25(18):4078. doi:10.3390/molecules25184078
- Massuela DC, Hartung J, Munz S, Erpenbach F, Graeff-hönninger S. Impact of harvest time and pruning technique on total CBD concentration and yield of medicinal cannabis. *Plan Theory.* 2022;11(1):140. doi:10.3390/plants11010140
- Citti C, Linciano P, Panseri S, et al. Cannabinoid profiling of hemp seed oil by liquid chromatography coupled to high-resolution mass spectrometry. *Front Plant Sci.* 2019;10:120. doi:10.3389/fpls.2019.00120
- European Monitoring Centre for Drugs and Drug Addiction. Low-THC cannabis products in Europe, Publ Off Eur Union 2020:19. doi:10.2810/69625
- European Monitoring Centre for Drugs and Drug Addiction. Medical use of cannabis and cannabinoids: questions and answers for policy-marking. Lisbon, 2018. Accessed September 21, 2022. https://www.emcdda.europa.eu/system/files/publications/10171/20185584_TD0618186FRN.pdf
- Health Europa. First CBD oil to be approved by the European Medicines Agency; 2019. Accessed September 21, 2022. <https://www.healtheuropa.com/cbd-oil-approved-european-medicines-agency>
- Hazekamp A. The trouble with CBD oil. *Med Cannabis Cannabinoids.* 2018;1(1):65-72. doi:10.1159/000489287
- Food and Drug Administration. Regulation of Cannabis and Cannabis-derived products, including cannabidiol (CBD); 2021. Accessed September 21, 2022. <https://www.fda.gov/news-events/public-health-focus/fda-regulation-cannabis-and-cannabis-derived-products-including-cannabidiol-cbd>
- Romano L, Hazekamp A. Cannabis oil: chemical evaluation of an upcoming cannabis-based medicine. *Cannabinoids.* 2013;1(1):1-11. doi:10.1159/000489363
- Carcieri C, Tomasello C, Simiele M, et al. Cannabinoids concentration variability in cannabis olive oil galenic preparations. *J Pharm Pharmacol.* 2018;70(1):143-149. doi:10.1111/jphp.12845
- Calvi L, Pentimalli D, Panseri S, et al. Comprehensive quality evaluation of medical *Cannabis sativa* L. inflorescence and macerated oils based on HS-SPME coupled to GC - MS and LC-HRMS (q-exactive orbitrap[®]) approach. *J Pharm Biomed Anal.* 2018;150(20):208-219. doi:10.1016/j.jpba.2017.11.073
- Kosovic E, Sykora D, Kuchar M. Stability study of cannabidiol in the form of solid powder and sunflower oil solution. *Pharmaceutics.* 2021;13(3):412. doi:10.3390/pharmaceutics13030412
- Fernández N, Carreras LJ, Larcher RA, Ridolfi AS, Quiroga PN. Quantification of cannabinoids in cannabis oil using GC/MS: method development, validation, and application to commercially available preparations in Argentina. *Planta Medica Int Open.* 2020;7(02):e81-e87. doi:10.1055/a-1155-6613
- Cardenia V, Gallina Toschi T, Scappini S, Rubino RC, Rodriguez-Estrada MT. Development and validation of a fast gas chromatography/mass spectrometry method for the determination of cannabinoids in *Cannabis sativa* L. *J Food Drug Anal.* 2018;26(4):1283-1292. doi:10.1016/j.jfda.2018.06.001

20. Duchateau C, Kauffmann J-M, Canfyn M, Stévigny C, De Braekeleer K, Deconinck E. Discrimination of legal and illegal *Cannabis* spp. according to European legislation using near infrared spectroscopy and chemometrics. *Drug Test Anal.* 2020;12(9):1309-1319. doi:10.1002/dta.2865
21. Deidda R, Coppey F, Damergi D, et al. New perspective for the in-field analysis of cannabis samples using handheld near-infrared spectroscopy: a case study focusing on the determination of Δ^9 -tetrahydrocannabinol. *J Pharm Biomed Anal.* 2021;202:114150. doi:10.1016/j.jpba.2021.114150
22. De Bruyne S, Speeckaert MM, Delanghe JR. Applications of mid-infrared spectroscopy in the clinical laboratory setting. *Crit Rev Clin Lab Sci.* 2018;55(1):1-20. doi:10.1080/10408363.2017.1414142
23. Cozzolino D. Near infrared spectroscopy in natural products analysis. *Planta Med.* 2009;75(07):746-756. doi:10.1055/s-0028-1112220
24. Jiménez-Carvelo AM, Osorio MT, Koidis A, González-Casado A, Cuadros-Rodríguez L. Chemometric classification and quantification of olive oil in blends with any edible vegetable oils using FTIR-ATR and Raman spectroscopy. *LWT.* 2017;86:174-184. doi:10.1016/j.lwt.2017.07.050
25. Coates J. A review of sampling methods for infrared spectroscopy—liquids. *Appl Spectrosc.* 1998;49-91. doi:10.1016/B978-012764070-9/50005-6
26. Li X, Zhang L, Zhang Y, et al. Review of NIR spectroscopy methods for nondestructive quality analysis of oilseeds and edible oils. *Trends Food Sci Technol.* 2020;101:172-181. doi:10.1016/j.tifs.2020.05.002
27. Chen Z, De Boves Harrington P, Griffin V, Griffin R. In situ determination of cannabidiol in hemp oil by near-infrared spectroscopy. *J Nat Prod.* 2021;84(11):2851-2857. doi:10.1021/acs.jnatprod.1c00557
28. Mishra P, Roger J-M, Jouan-Rimbaud-Bouveresse D, et al. Recent trends in multi-block data analysis in chemometrics for multi-source data integration. *TrAC Trends Anal Chem.* 2021;137:116206. doi:10.1016/j.trac.2021.116206
29. Health Europa – Medical Cannabis Network. Full-spectrum CBD oil: everything you need to know; 2022. Accessed October 27, 2022. <https://www.healtheuropa.com/full-spectrum-cbd-oil-everything-you-need-to-know/116269/>
30. Vujasinovic V, Djilas S, Dimic E, Romanic R, Takaci A. Shelf life of cold-pressed pumpkin (*Cucurbita pepo* L.) seed oil obtained with a screw press. *J Am Oil Chem Soc.* 2010;87(12):1497-1505. doi:10.1007/s11746-010-1630-x
31. UF IFAS extension, University of Florida. Health benefits of olive oil and olive extracts. Accessed April 19, 2022. <https://edis.ifas.ufl.edu/publication/FS282>
32. Da Porto C, Decorti D, Tubaro F. Fatty acid composition and oxidation stability of hemp (*Cannabis sativa* L.) seed oil extracted by supercritical carbon dioxide. *Ind Crop Prod.* 2012;36(1):401-404. doi:10.1016/j.indcrop.2011.09.015
33. Deferne J-L, Pate D. Hemp seed oil: a source of valuable essential fatty acids. *J Int Hemp Assoc.* 1996;3(1):4-7.
34. Superior Health Council. Oil and fat safety. Brussel, 2011. Accessed May 19, 2023. https://www.health.belgium.be/sites/default/files/uploads/fields/fpshealth_theme_file/19067528/S%C3%A9curit%C3%A9%20des%20huiles%20et%20des%20graisses%20%28janvier%202011%29%20%28CSS%208310%29.pdf
35. Duchateau C, Canfyn M, Desmedt B, et al. CBD oils on the Belgian market: a validated MRM GC-MS/MS method for routine quality control using QuEChERS sample clean up. *J Pharm Biomed Anal.* 2021;205:114344. doi:10.1016/j.jpba.2021.114344
36. Márquez C, López MI, Ruisánchez I, Callao MP. FT-Raman and NIR spectroscopy data fusion strategy for multivariate qualitative analysis of food fraud. *Talanta.* 2016;161:80-86. doi:10.1016/j.talanta.2016.08.003
37. Westerhuis JA, Kourti T, MacGregor JF. Analysis of multiblock and hierarchical PCA and PLS models. *J Chemometr.* 1998;12(5):301-321. doi:10.1002/(sici)1099-128x(199809/10)12:5%3C301::aid-cem515%3E3.3.co;2-j
38. Bro R, Smilde AK. Principal component analysis. *Anal Methods.* 2014;6(9):2812-2831. doi:10.1039/c3ay41907j
39. Abdi H, Williams L. Principal component analysis. *Wiley Interdiscip Rev Comput Stat.* 2010;2(4):433-459. doi:10.1002/wics.101
40. Pomerantsev AL, Rodionova OY. Popular decision rules in SIMCA: critical review. *J Chemometr.* 2020;34(8):1-14. doi:10.1002/cem.3250
41. Mevik B-H, Wehrens R. Introduction to the pls package. Help Sect “PLS” Packag RStudio Softw 2015; 1–23.
42. Siano F, Moccia S, Picariello G, et al. Comparative study of chemical, biochemical characteristic and ATR-FTIR analysis of seeds, oil and flour of the edible Fedora cultivar hemp (*Cannabis sativa* L.). *Molecules.* 2018;24(1):1-13. doi:10.3390/molecules24010083
43. Ledoux M. Main constituents of lipids structure, classification and chemical nomenclature- Direction de l'Evaluation des Risques Observatoire Nutritionnelle des Aliments. Centre for Research and Nutritional Information (CERIN) 2012; 132–133. <https://www.cerin.org/wp-content/uploads/2012/12/132-133-principaux-constituants.pdf>
44. Volmajer Valh J, Peršin Z, Vončina B, Vrezner K, Tušek L, Fras Zemljčič L. Microencapsulation of cannabidiol in liposomes as coating for cellulose for potential advanced sanitary material. *Coatings.* 2021;11(1):3. doi:10.3390/coatings11010003
45. Sánchez-Carnero Callado C, Núñez-Sánchez N, Casano S, Ferreira-Vera C. The potential of near infrared spectroscopy to estimate the content of cannabinoids in *Cannabis sativa* L.: a comparative study. *Talanta.* 2018;190:147-157. doi:10.1016/j.talanta.2018.07.085

How to cite this article: Duchateau C, Stévigny C, De Braekeleer K, Deconinck E. Characterization of CBD oils, seized on the Belgian market, using infrared spectroscopy: Matrix identification and CBD determination, a proof of concept. *Drug Test Anal.* 2023;1-15. doi:10.1002/dta.3583